Journal of Applied Fluid Mechanics, Vol. 13, No. 3, pp. 935-943, 2020.
Available online at www.jafmonline.net, ISSN 1735-3572, EISSN 1735-3645.
DOI: 10.29252/jafm.13.03.30618

Universal Method for Determination of Leakage in Labyrinth Seal

D. Joachimiak

Chair of Thermal Engineering, Poznan University of Technology, Poznań, 60-965 Poznań, Poland

†*Corresponding Author Email: damian.joachimiak@put.poznan.pl*

(Received June 12, 2019; accepted November 5, 2019)

ABSTRACT

This paper presents calculation model enabling determination of the leakage rate in labyrinth seals. Described model is based on the Saint-Venant equation. It includes a new type of flow coefficient, which was determined based on experimental tests and described depending on the Reynolds number and the radial clearance. The structure of this calculation model can be applied to determine the leakage rate in straight through, staggered labyrinth seals as well as with various number of clearances. This model enables determining distribution of thermodynamic and flow parameters of the gas along the seal length. Results obtained from this model were next compared with experimental data for various types of seals. It enabled determination of kinetic energy carry-over coefficient in geometries under investigation. The value of this coefficient was then compared with the value of the coefficient from the Scharrer's, Neumann's and Hodkinson's models. Obtained results indicate that the value of the kinetic energy carry-over coefficient depends not only on the seal geometry, but also on the pressure decrease.

Keywords: Labyrinth seal; Leakage; Calculation model; Experiment; Flow coefficient; Kinetic energy carry-over.

NOMENCLATURE

A	clearance flow area
B	teeth thickness
c	critical parameter
c	flow coefficient
C	value referring to the clearance
D	diameter of the seal
e	value obtained during the experiment
H	height of the seal segment
H	value obtained from the Hodkinson's model
i1	diameter of the first inner clearance of the staggered seal
i2	diameter of the second inner clearance of the staggered seal
LP	length of the pitch
LS	length of the segment
max	maximum value
N	value obtained from the Neumann's model
o1	diameter of the first outer clearance of the staggered seal
o2	diameter of the second outer clearance of the staggered seal
p	absolute pressure
RC	radial clearance
Re	Reynolds number
S	value obtained from the Scharrer's model
Subscripts	
SV	theoretical value from the Saint-Venant equation
t	number of teeth
T	temperature
u	axial velocity
v	specific volume
$\dot{m}$	mass flow
01	total parameter upstream the clearance
2	static parameter downstream the clearance
2s	value being the result of the isentropic change
β	pressure ratio
γ	kinetic energy carry-over coefficient
δ	relative error
κ	isentropic exponent
μ	dynamic viscosity
ρ	density
Ψ	flow number

1. INTRODUCTION

Labyrinth seals affect significantly the effectiveness of fluid-flow machines. Nowadays, there are numerous calculation models taking into consideration flow coefficients which enable leakage estimation. One of the first models describing gas flow in a seal, which included constant flow coefficient, was developed by Martin (1908). Other scientists, Egli (1935), Hodkinson (1939), Zimmerman and Wolff (1987), included to their models empirically determined flow coefficient and the phenomenon of kinetic energy carry-over. Another type of calculation models, in which the flow in a seal is analyzed tooth-by-tooth, was initialized by Neumann Childs and Scharrer (1988) and Scharrer (1988). In their models, the flow coefficient is a function of pressure distribution in the seal, and the kinetic energy carry-over coefficient depends on the seal geometry. In the reference paper Melnik (2013), the modified Stodola method was used to determine the leakage of compressible and incompressible liquids in the straight through labyrinth seal. Presented model was transformed to be used in calculations for groove seals. Another group of calculation models are models based on friction coefficients determined experimentally for a specific seal geometry. Modified Neumann method and Moody's friction-factor model were used in reference paper Dereli and Eser (2004). This allows the authors to determine the leakage value, the pressure distribution and the distribution of gas velocity in chambers of the straight through labyrinth seal. Gas flow in a short labyrinth seal for relatively small pressure drops was described with the use of a model based on the friction coefficient, Zhirong *et al.* (2015). This coefficient was determined based on experimental data. Presented model accurately reflects the value of leakage for a specific type of sealing. Model describing the gas flow in the cavity seal based on the enthalpy balance equation is presented in the paper by Joachimiak and Krzyślak (2016). In this model, the gas kinetic energy dissipation into heat, being the result of the friction between the gas and the wall, was taken into consideration. Friction was investigated as the modified coefficient based on the Blasius' equation. In their paper Hu *et al.* (2014), described the flow characteristics of straight through and stepped labyrinth seals using the friction coefficient. It was described by functions of Reynolds and Mach numbers, the equivalent diameter and the seal length. Similar models are also used in (Hong *et al.* 2012, Kawashima and Asako 2014, Asako *et al.*2005) for describing the gas flow in mini-channels.

Models enabling the determination of the pressure drop in the straight through labyrinth seal were presented in the paper by Asok *et al.* (2007). Analysis concerned the relation between the chamber size, the teeth shape and the leakage. The paper presented semi-theoretical model based on two coefficients of virtual cavity velocity and the vortex loss coefficient.

Leak-tightness of the seal depends on such features of the seal geometry as pitch, length and height of the chamber (Zhang *et al.* 2014, (Yuan *et al.* 2015), Wang *et al.* 2007, Joachimiak and Krzyślak 2019, Szymanski *et al.* 2018, Lampart, 2009). Of significant impact on the seal leak-tightness is its wear, Joachimiak and Krzyślak (2017).

Calculation model which can be applied in a straight, staggered seal is presented in this paper. In part one of this paper, a method for determining the flow coefficient c_{SV} based on experimental tests for the model gas flow through one clearance is presented. This coefficient was defined as the ratio of gas mass flow obtained from the experiment to gas mass flow resulting from the Saint-Venant equation. Next part of this paper comprises the description of the calculation model based on the Saint-Venant equation. This model includes the flow coefficient c_{SV}, which in turn enables the real flow conditions occurring in clearances of multi-tooth seals to be taken into consideration. The last part of this paper includes results of the experimental tests and of calculations made with the use of the model for straight and staggered seals of various number of teeth. The kinetic energy carryover coefficient γ for geometries being investigated was determined.

2. STAND FOR EXPERIMENTAL TESTS

Experimental tests were conducted on the test stand shown in Fig. 1. Test stand (Fig. 1.) consists of a compressor, a main tank, a regulator valve and the sealing system. Sealing system consists of the body and the insert (internal part) placed centrically in the body on which the investigated geometry is located.

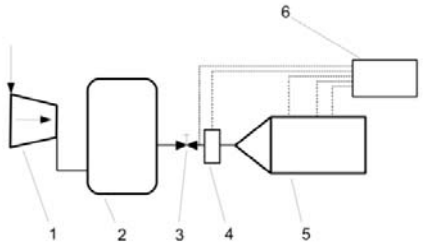

Fig. 1. Diagram of a test stand for labyrinth seals, 1 - compressor, 2 - main tank, 3 - regulator valve, inlet channel, 4 - orifice, 5 – body with labyrinth seal, 6 – measurement system.

The measurement of the mass flow was performed with the use of an orifice. Measuring stand was equipped with the absolute pressure transmitters having the measurement range of 0-5x10^5 Pa and the measuring accuracy of ±0.25% as well as with pressure difference transmitters having the measurement range of 0-0.25x10^5 Pa and the measuring accuracy of ±0.2%. Gas temperature was measured by T-type thermocouples.

3. METHOD FOR DETERMINING THE FLOW COEFFICIENT BASED ON EXPERIMENTAL TESTS

To determine the flow coefficient for labyrinth

seals, some experimental tests were conducted on a model geometry composed of one tooth with a radial clearance of *RC* (Fig. 2).

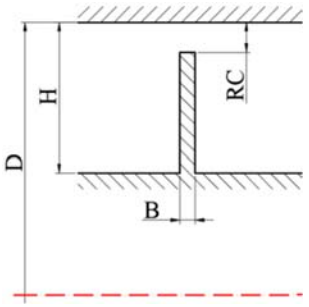

Fig. 2. Geometry of the representative gap for determining the coefficient c_{SV}.

Mass flow, pressure and gas temperature upstream and downstream the clearance were measured during the experiment. Dimensions of the analyzed radial clearances are summarized in table 1.

Table 1 Geometry dimensions

Mark	Name	Size [mm]
D	Diameter of the seal	150
H	Height of the seal segment	10
B	Disc thickness	1
RC	Radial clearance	0.362 0.542 0.752 1.067 1.5485 2.058

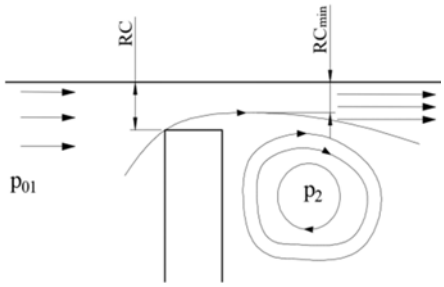

Fig. 3. Scheme of gas flow in the annular gap, *RC* – radial clearance, RC_{min} – minimum cross-section of the gas flow.

The flow coefficient takes into consideration phenomena occurring at the inflow to the clearance (gas acceleration), in the clearance (occurrence of boundary layer on the surface of the body and at the tooth back, flow contraction) and phenomena occurring downstream the clearance (formation of the gas flux of a high velocity and the occurrence of dissipation vortex behind the tooth).

Mass flow flowing through the annular clearance depends on total parameters of gas upstream the gap p_{01}, T_{01} and the static pressure in the space downstream the gap p_2. One of the parameters describing the mass flow is the pressure ratio upstream and downstream the clearance determined as:

$$\beta = \frac{p_2}{p_{01}} \tag{1}$$

Theoretical mass flow is determined by the Saint-Venant equation (Trütnovsky, 1964)

$$\dot{m}_{SV} = A_C \Psi \sqrt{p_{01}\rho_{01}} \tag{2}$$

where the surface area of the flow in the clearance can be determined as

$$A_C = \frac{\pi}{4}\left[D^2 - \left(D - 2RC\right)^2\right] \tag{3}$$

Equation (2) includes the flow number Ψ (Trütnovsky, 1964), value of which depends on the type of the gas. Gas is described by the isentropic exponent κ and gas constant R. For the subcritical air flow, $\beta > 0.5283$. flow number is of the form (Trütnovsky, 1964)

$$\Psi = \sqrt{2\frac{\kappa}{\kappa\text{-}1}\left[\left(\beta\right)^{\frac{2}{\kappa}} - \left(\beta\right)^{\frac{\kappa+1}{\kappa}}\right]} \tag{4a}$$

For the supercritical flow, $\beta \le 0.5283$

$$\Psi = \sqrt{\kappa\left(\frac{2}{\kappa+1}\right)^{\frac{\kappa+1}{\kappa\text{-}1}}} \tag{4b}$$

Flow coefficient for gas flowing through the clearance was defined as the ratio of mass flow obtained from the experiment $\dot{m}_e$ to mass flow resulting from the Saint-Venant equation $\dot{m}_{SV}$ (2)

$$c_{SV} = \frac{\dot{m}_e}{\dot{m}_{SV}} \tag{5}$$

Mass flow determined by the Saint-Venant equation depends on, among other, total parameters of gas upstream the clearance and on static parameters downstream the clearance. To apply the coefficient c_{SV} in multi-tooth segments, one should know the total pressure before each tooth and the static pressure behind each tooth. To determine these pressures, one should analyze flow conditions in each chamber and in each clearance. If one-dimensional models are used, there arises a problem in which the variation of thermodynamic and flow parameters along the segment length should be determined.

We propose in this paper a variation of the flow coefficient depending on the Reynolds number and the radial clearance *RC*.

$$c_{SV} = f\left(Re, RC\right) \tag{6}$$

Reynolds number is related to thermodynamic parameters of gas at the outflow from the clearance, with the assumption of the isentropic change

$$Re = \frac{2RCu}{\mu v_{01}\left(\frac{p_{01}}{p_2}\right)^{\frac{1}{\kappa}}} \tag{7}$$

where the gas velocity in the clearance is determined from the Saint-Venant equation

$$u = \left[2\frac{\kappa}{\kappa\text{-}1}p_{01}v_{01}\left[1-\left(\frac{p_2}{p_{01}}\right)^{\frac{\kappa-1}{\kappa}}\right]\right]^{0.5}. \tag{8}$$

Values of the flow coefficient c_{SV} were determined for the clearance heights under consideration (table 1) based on experimental tests.

4. Results Of Experimental Tests Of Flow Coefficient c_{SV}

In this paper, we present a method of determining the flow coefficient for conditions where gas flowing into the clearance has negligible velocity. In this situation, the gas velocity in the clearance results from the pressure gradient. This creates ideal conditions of gas flow in the clearance being characterized by the lowest mass flow. Obtained values of the flow coefficient for the geometry described in table 1 are presented in the function of the Reynolds number (Fig. 4).

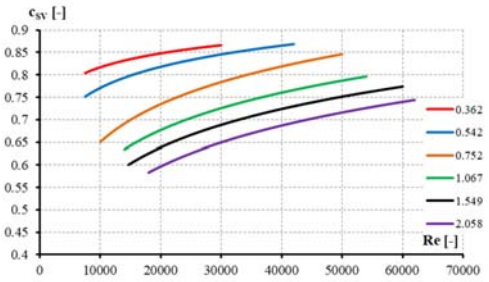

Fig. 4. Values of the flow coefficient c_{SV} in the function of the Reynolds number for radial clearances RC from 0.362 to 2.058 mm.

The flow coefficient has the highest value for the radial clearance of 0.362 mm. For greater clearances, flow coefficients c_{sv} reach increasingly lower values.

Each curve presented in Fig. 4 was approximated by the polynomial of the following form

$$c_{SV} = \sum_k a_k (Re)^k \tag{9}$$

The determined flow coefficient c_{SV} was next applied in the model described below.

5. CSV Calculation Model

Calculation model is based on the Saint-Venant equation (Joachimiak *et al.* 2012). This equation determines the mass flow flowing through i-th clearance

$$\dot{m}_i = A_{Ci}\left[2\frac{\kappa}{\kappa\text{-}1}\frac{p_i}{v_i}\left\{\left(\frac{p_{i+1}}{p_i}\right)^{\frac{2}{\kappa}}-\left(\frac{p_{i+1}}{p_i}\right)^{\frac{1+\kappa}{\kappa}}\right\}\right]^{0.5} \tag{10}$$

where the flow surface area in i-th clearance is described by the formula

$$A_{Ci} = \frac{\pi}{4}\left[D_i^2-\left(D_i^2-2RC_i\right)^2\right] \tag{11}$$

After the function of the mass flow $\dot{m}_i(p_i, p_{i+1})$ (Eq. 10) is expanded into the Taylor series for the pressure $(\tilde{p}_i, \tilde{p}_{i+1})$ relative to the pressure upstream the tooth p_i and downstream the tooth p_{i+1}, we have

$$\dot{m}_i(p_i,p_{i+1}) = \dot{m}_i(\tilde{p}_i,\tilde{p}_{i+1}) + \frac{(p_i-\tilde{p}_i)}{1!}\frac{\partial \dot{m}_i}{\partial p_i} + \frac{(p_{i+1}-\tilde{p}_{i+1})}{1!}\frac{\partial \dot{m}_i}{\partial p_{i+1}} + \frac{(p_i-\tilde{p}_i)^2}{2!}\frac{\partial^2 \dot{m}_i}{\partial p_i^2} + \frac{(p_i-\tilde{p}_i)(p_{i+1}-\tilde{p}_{i+1})}{1!1!}\frac{\partial^2 \dot{m}_i}{\partial p_i \partial p_{i+1}} + \frac{(p_{i+1}-\tilde{p}_{i+1})^2}{2!}\frac{\partial^2 \dot{m}_i}{\partial p_{i+1}^2} + \ldots =$$

$$= \dot{m}_i(\tilde{p}_i,\tilde{p}_{i+1}) + \sum_{k=1}^{n}\sum_{l=0}^{k}\frac{(p_i-\tilde{p}_i)^{k-l}(p_{i+1}-\tilde{p}_{i+1})^l}{(k-l)!l!}\times \frac{\partial^{(k-l)}\dot{m}_i}{\partial p_i^{(k-l)}}\frac{\partial^l \dot{m}_i}{\partial p_{i+1}^l} + R_n \tag{12}$$

In further analysis the approximation of the function $\dot{m}_i(p_i, p_{i+1})$ to first derivatives was used. Ignoring derivatives of higher order, having significantly lower values than the first order derivatives, results in linearization of the Sain-Venant equation (Eq. (10)), which can be noted in the following form

$$\dot{m}_i(p_i,p_{i+1}) \approx \dot{m}_i(\tilde{p}_i,\tilde{p}_{i+1}) + \frac{(p_i-\tilde{p}_i)}{1!}\frac{\partial \dot{m}_i}{\partial p_i} + \frac{(p_{i+1}-\tilde{p}_{i+1})}{1!}\frac{\partial \dot{m}_i}{\partial p_{i+1}} \tag{13}$$

Hence, after transferring $\dot{m}_i(\tilde{p}_i, \tilde{p}_{i+1})$ to the left-handed side of the Eq. (13), we have

$$\dot{m}_i(p_i,p_{i+1}) - \dot{m}_i(\tilde{p}_i,\tilde{p}_{i+1}) \approx \frac{(p_i-\tilde{p}_i)}{1!}\frac{\partial \dot{m}_i}{\partial p_i} + \frac{(p_{i+1}-\tilde{p}_{i+1})}{1!}\frac{\partial \dot{m}_i}{\partial p_{i+1}} \tag{14}$$

Equation (14) describes the change of the mass flow of gas flowing through i-th clearance $\dot{m}_i(p_i, p_{i+1}) - \dot{m}_i(\tilde{p}_i, \tilde{p}_{i+1})$ resulting from the change in the pressure upstream $p_i - \tilde{p}_i$ and downstream $p_{i+1} - \tilde{p}_{i+1}$ clearances. This dependence can be noted as exact differential of the mass flow in i-th clearance relative to the pressure upstream p_i and downstream p_{i+1} clearances:

$$d\dot{m}_i = \frac{\partial \dot{m}_i}{\partial p_i} dp_i + \frac{\partial \dot{m}_i}{\partial p_{i+1}} dp_{i+1} \tag{15}$$

Partial derivatives included in Eq. (15) are of the following form:

$$\frac{\partial \dot{m}_i}{\partial p_i} = \frac{A_{Ci}}{2}\left(\frac{2\kappa\text{-}2}{\kappa} p_i^{\frac{\kappa\text{-}2}{\kappa}} p_{i+1}^{\frac{2}{\kappa}} - \frac{\kappa+1}{\kappa} p_i^{\frac{1}{\kappa}} p_{i+1}^{\frac{\kappa+1}{\kappa}} \right) \times \sqrt{\frac{2\frac{\kappa}{\kappa\text{-}1}\frac{1}{T_0 \mathrm{R}}}{p_i^{\frac{2\kappa\text{-}2}{\kappa}} p_{i+1}^{\frac{2}{\kappa}} - p_i^{\frac{\kappa+1}{\kappa}} p_{i+1}^{\frac{\kappa+1}{\kappa}}}}, \tag{16}$$

$$\frac{\partial \dot{m}_i}{\partial p_{i+1}} = \frac{A_{Ci}}{2}\left(\frac{2}{\kappa} p_i^{\frac{2\kappa\text{-}2}{\kappa}} p_{i+1}^{\frac{2\text{-}\kappa}{\kappa}} - \frac{\kappa+1}{\kappa} p_i^{\frac{\kappa+1}{\kappa}} p_{i+1}^{\frac{1}{\kappa}} \right) \times \sqrt{\frac{2\frac{\kappa}{\kappa\text{-}1}\frac{1}{T_0 \mathrm{R}}}{p_i^{\frac{2\kappa\text{-}2}{\kappa}} p_{i+1}^{\frac{2}{\kappa}} - p_i^{\frac{\kappa+1}{\kappa}} p_{i+1}^{\frac{\kappa+1}{\kappa}}}}. \tag{17}$$

Equation (15) describes the change in the mass flow flowing through the clearance resulting from the change in pressure upstream and downstream the clearance. Equation (15), transformed to finite increments, has the following form:

$$\Delta \dot{m}_i = \frac{\partial \dot{m}_i}{\partial p_i} \Delta p_i + \frac{\partial \dot{m}_i}{\partial p_{i+1}} \Delta p_{i+1} \tag{18}$$

Vector of differences between finite increments of mass flows can be written as follows:

$$\Delta \dot{m}_i - \Delta \dot{m}_{i+1} = \frac{\partial \dot{m}_i}{\partial p_i} \Delta p_i + \left(\frac{\partial \dot{m}_i}{\partial p_{i+1}} - \frac{\partial \dot{m}_{i+1}}{\partial p_{i+1}} \right) \Delta p_{i+1} - \frac{\partial \dot{m}_{i+1}}{\partial p_{i+2}} \Delta p_{i+2} \tag{19}$$

for $i = 1, \ldots, n-1$

Based on the system (n – 1) of Eq. (19), the system of linear equations can be created as

$$\mathbf{C}\Delta\mathbf{p} = \Delta\dot{\mathbf{M}} \tag{20}$$

where

$$C_{i,j} = \left(\frac{\partial \dot{m}_i}{\partial p_{i+1}} - \frac{\partial \dot{m}_{i+1}}{\partial p_{i+1}} \right) \tag{21}$$

for $j = i$ and $i = 1, 2, \ldots, n\text{-}1$

$$C_{i,j} = -\frac{\partial \dot{m}_{i+1}}{\partial p_{i+2}} \tag{22}$$

for $j = i+1$ and $i = 1, 2, \ldots, n\text{-}2$

$$C_{i,j} = \frac{\partial \dot{m}_i}{\partial p_i} \tag{23}$$

for $j = i - 1$ and $i = 2, 3, \ldots, n\text{-}1$.

Remaining elements of the matrix **C** are zero.

From Eq. (19), the vector of pressure increments **Δp**

$$\Delta\mathbf{p} = \left[\Delta p_1 \quad \Delta p_2 \quad \ldots \quad \Delta p_{n-1} \right]^T \tag{24}$$

where $\Delta p_i = p_i - p_{i+1}$.

as well as the vector of mass flow differences

$$\Delta\dot{\mathbf{M}} = \left[\Delta\dot{\mathrm{M}}_1 \quad \Delta\dot{\mathrm{M}}_2 \quad \ldots \quad \Delta\dot{\mathrm{M}}_{n-1} \right]^T \tag{25}$$

were isolated.

Vector of mass flow differences is determined based on Eq. (10).

$$\Delta\dot{\mathbf{M}}_i = \Delta\dot{m}_i - \Delta\dot{m}_{i+1} \tag{26}$$

To determine the vector of pressure increments **Δp**, some iterative calculations are carried out.

In the first iteration, a linear distribution of pressure **p** is assumed. In subsequent iterations, the vector **p** is corrected by the resultant vector of pressure increments **Δp.** Distribution of pressure **p** rearranges itself so that there exist the same mass flow in each clearance.

In the next step of the iterative process, vectors **u** and **Re** described by the following formulae

$$u_i = \left[2\frac{\kappa}{\kappa\text{-}1} p_i v_i \left\{ 1 - \left(\frac{p_{i+1}}{p_i} \right)^{\frac{\kappa\text{-}1}{\kappa}} \right\} \right]^{0.5} \tag{27}$$

$$Re_i = \frac{2RC_i u_i}{\mu v_i \left(\frac{p_i}{p_{i+1}} \right)^{\frac{1}{\kappa}}} \tag{28}$$

are generated.

For each clearance, the flow coefficient c_{SV} which depends on radial clearance and the Reynolds number is determined. This coefficient is described by formula (9). For radial clearances other than those given in table 1, the coefficient c_{SV} is interpolated.

Vector of mass flow differences in Eq. (25) is corrected by the vector of flow coefficients $\mathbf{c}_{\mathrm{SV}}$.

$$\Delta\dot{\mathbf{M}}_i = c_{\mathrm{SV}\,i}\dot{m}_i - c_{\mathrm{SV}\,i+1}\dot{m}_{i+1} \tag{29}$$

Iterative calculations are completed when the highest value of the component of the relative differences of mass flow vector is lower than or equal to the assumed accuracy of calculations ε

$$\max_i \left| \delta\dot{\mathbf{M}}_i \right| = \max_i \frac{\left| \dot{m}_{i+1} - \dot{m}_i \right|}{\dot{m}_{i+1}} \le \varepsilon \tag{30}$$

This model is programmed in the Fortran language.

Presented model with the flow coefficient c_{SV} includes real flow conditions in seal clearances. Ideal conditions for gas velocity reduction in seal chambers are assumed in this model. It allows to determine the minimum theoretical value of leakage in seals of various geometries for radial clearance ranging from 0.362 to 2.058 mm. The advantage of the presented model is the fact that it can be used to determine theoretical value of leakage in the straight through and staggered seals where gas is flowing into axial direction. In the next part of this

paper results obtained from the CSV model and from experimental tests are compared with results obtained from other models described in source literature.

6. Analysis Of Experimental Tests And Calculations Results

Model CSV described herein includes conditions of gas flow through the clearance, presented by the coefficient c_{SV}. In real conditions, the gas velocity in the labyrinth seal upstream the gap is higher than the velocity assumed in model tests (Chapter 3). It results from the gas expansion in the preceding gap and incomplete dissipation of kinetic energy in the chamber upstream the gap. Hence, the mass flow for multi-tooth seals obtained from the experiment $\dot{m}_e$ should be higher than the one obtained from the model CSV $\dot{m}_{CSV}$.

$$\dot{m}_e \geq \dot{m}_{CSV} \tag{31}$$

Calculation model presented in this paper enables determining the kinetic energy carry-over coefficient γ_{CSV} between the gaps. This coefficient is defined as the ratio of the mass flow obtained from the experiment to the mass flow from the model CSV

$$\gamma_{CSV} = \frac{\dot{m}_e}{\dot{m}_{CSV}} \tag{32}$$

In the next part of the paper the coefficient γ_{CSV} obtained from the CSV model will be compared with Scharrer's, Neumann's and Hodkinson's models. The coefficient value in Scharrer's model is described by the following equation:

$$\gamma_S = \left(\frac{1}{(1-\alpha_{Si})} \right)^{0.5} \tag{33}$$

where $\alpha_S = \dfrac{8.52}{(LP-B)/RC + 7.23}$.

Coefficient in the Scharrer's model includes features of the seal geometry such as the radial clearance RC, pitch LP and the thickness of teeth B, whereas the value of the coefficient γ_N in the Neumann's model (Childs & Scharrer, 1986) depends on the pitch LP and the height of the clearance RC.

$$\gamma_N = \left(\frac{t}{t(1-\alpha_N)+\alpha_N} \right)^{0.5} \tag{34}$$

where $\alpha_N = 1-(1+16.6RC/LP)^{-2}$

The value of the kinetic energy carry-over coefficient γ_H in the Hodkinson's model (Hodkinson, 1939), similarly as in the Neumann's model, depends on the radial clearance and the length of the pitch.

$$\gamma_H = \left(\frac{1}{1-\dfrac{t-1}{t}\dfrac{RC/LP}{RC/LP+0.02}} \right)^{0.5} \tag{35}$$

Tests were conducted for the geometry of straight through seals of various number of teeth (Fig. 5 (a), Table 2) and for the staggered seals composed of twenty teeth (Fig. 5 (b), Table 3).

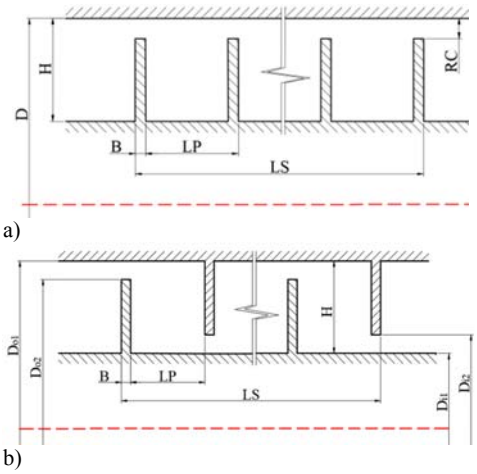

Fig. 5. Examined seal geometries a) straight through b) staggered.

In straight through seals, there occurs a high velocity of gas flowing through the upper part of the seal chambers which affects significantly the seal leakage. Staggered seals have more complicated geometry. Teeth of the staggered seal are placed on the shaft and on the body of the device. Such seals are characterized by lower gas velocity between gaps and more complicated gas swirl in chambers. That is why they are tighter than the straight through seals.

Table 2 Geometries of straight through segments of the radial clearance RC = 0.362, 0.542, 0.752 mm, being included in the experimental tests. Constant dimensions of the seal are: the diameter D = 150 mm, chambers height H = 10 mm and the thickness of teeth B = 1 mm

Geometry	Teeth number t	Pitch LP [mm]	Seal length LS [mm]
4t	4	10	31
6t	6	6	31
11t	11	3	31
4t_PL30_RC0.362	4	30	91

Values of the kinetic energy carry-over coefficients were determined based on the models described above and next compared with results obtained based on experimental tests and from calculations made with the use of CSV model. Figure 6 presents results for the straight through seal of the clearance

height of RC = 0.542 mm and the teeth number of 4, 6 and 11 (Table. 2).

Table 3 Geometries of staggered seals for teeth number t = 20, pitch LP = 10, thickness of teeth B=1 mm and chambers height H=10 mm and the seal length LS = 191 mm, being included in the experimental tests

Geometry	D_{o1} [mm]	D_{o2} [mm]	D_{i1} [mm]	D_{i2} [mm]
20t_RC0.5	120	138.98	139.93	120.97
20t_RC0.7	120	138.59	139.93	121.39
20t_RC1	120	137.99	139.93	121.99

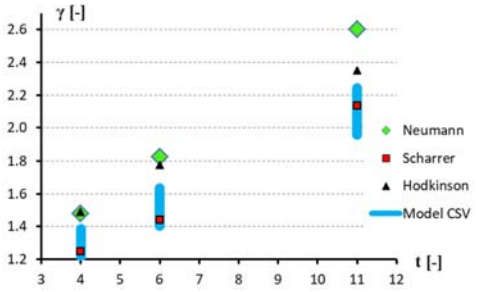

Fig. 6. Values of coefficients γ obtained from the analyzed models for segments of straight through seals having 4, 6 and 11 teeth.

Values of the kinetic energy carry-over coefficients obtained from the CSV model depend on the pressure p_{in}/p_{out} ratio. Therefore, in Fig. 6, values γ are presented by the range. It results from this figure that the number of seal teeth influences significantly on the γ value. The greater is the number of teeth, the shorter are chambers. It results in greater intensity of the kinetic energy carry-over which in turn causes the growth of γ. For the segment comprising 4 and 6 teeth, Neumann's and Hodkinson's models give comparable values of the kinetic energy carry-over coefficient.

Range of results from the CSV model include lower values than these obtained from the Neumann's model, Eq. (34), and the Hodkinson's one, Eq. (35). The value of the kinetic energy carry-over coefficient calculated with the use of the Scharrer's model, Eq. (33), is included in the range of results obtained from the CSV model. For the segment 11t, with short chambers, the highest value of γ was obtained from the Neumann's model and it amounted ca. 2.6. Slightly lower value was obtained from the Hodkinson's model, amounting to 2.35. Neumann's and Hodkinson's models brought extortionate values of the kinetic energy carry-over coefficient when compared with the Scharrer's model since they did not take into account the tooth thickness (Fig. 6).

Scharrer's model, unlike other models discussed herein, takes into account the tooth thickness what influences significantly on the accuracy of the determined coefficient γ. Therefore, it could be stated that it is the most precise model among these cited, which was also investigated in this paper (Joachimiak & Krzyślak, 2019). Values of the kinetic energy carry-over coefficient in the Scharrer's model for geometries 4, 6 and 11t are within the range of values obtained from the CSV model. Further in this paper coefficients γ obtained based on experiments and the CSV model will be compared with the Scharrer's model.

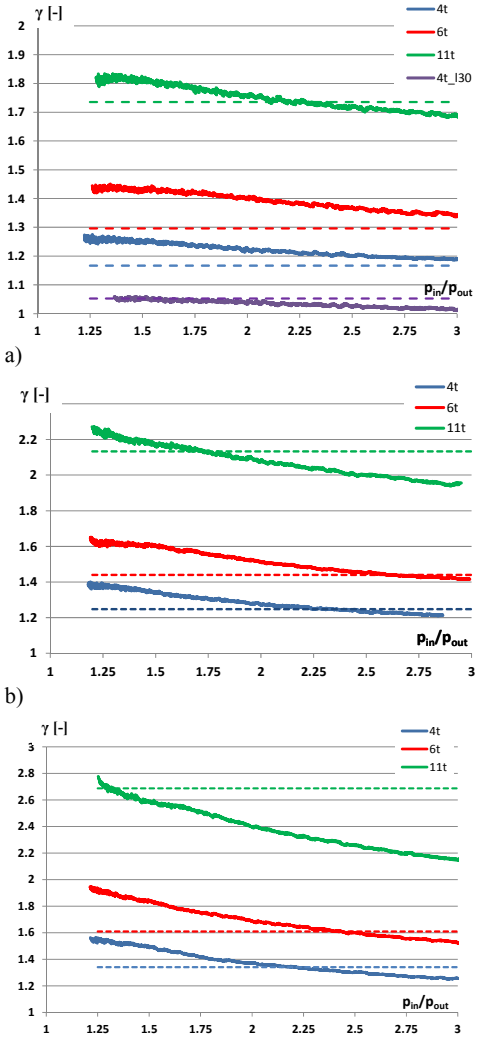

Fig. 7. Values of the kinetic energy carry-over coefficient γ for the straight through labyrinth seal of the number of teeth of 4, 6 and 11t for a) RC = 0.362, b) RC = 0.542, c) RC = 0.752 mm. Full line denotes data obtained from tests, broken line denotes data calculated as per Scharrer Eq. 33.

Figure 7 presents results obtained for straight through segments of the radial clearance RC = 0.362, 0.542 and 0.752 and of 4, 6, 11 teeth. The lower is the parameter γ, the better conditions for kinetic energy dissipation are observed in the given seal. For the straight through seals, the lower

boundary value of γ is 1. This value indicates that the kinetic energy is not carried over gaps of the seal. The value of γ close to 1 was obtained for the test geometry 4t_L30_RC0.362 (table 2), having the pitch of a significant length L = 30 mm (Fig. 7 (a)). When the parameter γ>1, it means that there is incomplete kinetic energy dissipation in chambers of the seal.

Values of the coefficient γ_{CSV} obtained from tests are similar to the value of the coefficient from the Scharrer's model (Fig. 7). In the latter model, values γ_S do not depend on the pressure ratio. For segments 4, 6, 11t of the analyzed radial clearances, the parameter γ_S has almost linear course. The lowest values of γ were obtained for four-tooth segments with the narrowest clearance.

Value of γ for a given number of teeth depends mainly on the extent of wear. The greater is the height of the clearance, the greater is value of γ, and the drop of γ in the function p_{in}/p_{out} is more noticeable (Fig. 6 (b), (c)). For geometries under consideration (4, 6 and 11t), the value of γ is affected significantly by the length of the seal pitch. The shorter is the pitch (Table. 2), the greater is the value of parameter γ. It results from the occurrence of high gas velocity between gaps. To estimate the change of γ_{CSV} of the investigated geometries depending on the clearance height, values of this coefficient (Fig. 8) were collated for the geometries 4-11t under consideration depending on the radial clearance RC for p_{in}/p_{out} = 2. Kinetic energy carry-over coefficient for geometry 4t ($\Delta\gamma$ = 0.15) increases slightly as a result of increasing radial clearance RC. Greater increase ($\Delta\gamma$ = 0.29) was observed for geometry 6t, and the greatest one – for geometry 11t of the smallest pitch ($\Delta\gamma$ = 0.64), what is presented in Fig. 8.

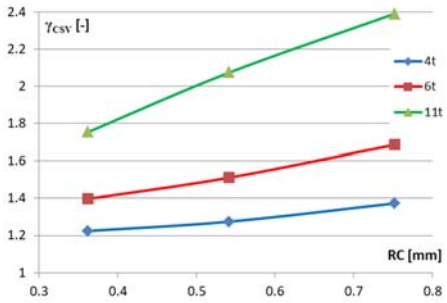

Fig. 8. Kinetic energy carry-over coefficient γ_{CSV} for seal of 4, 6 and 11t teeth depending on the radial clearance RC for the pressure ratio p_{in}/p_{out} = 2.

Figure 9 presents values of the kinetic energy carry-over coefficient for a staggered seal composed of twenty teeth. Parameter γ_{CSV} for the segment 20t_RC0.5 is almost constant in the investigated range of pressure drop and amounts approx. 1.4. Respectively, for clearances 0.752 and 1, the parameter γ_{CSV} has increasingly lower values.

In the case of the staggered seal, for the greater radial clearance (RC = 0.5, 0.7 and 1 mm), reduction of the parameter γ_{CSV} was observed, hence the effect of kinetic energy carry-over decreases (Fig. 9).

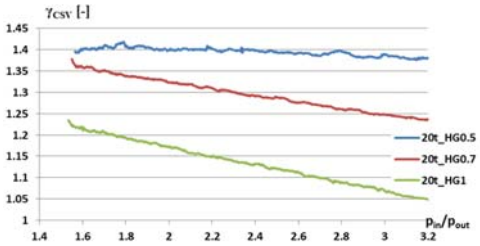

Fig. 9. Values of the kinetic energy carry-over coefficient γ for the staggered labyrinth seal composed of twenty teeth depending on the pressure ratio p_{in}/p_{out} for RC = 0.5, 0.7 and 1 mm.

7. CONCLUSION

The presented calculation model is based on the Saint-Venant equation. It includes experimentally determined flow coefficient c_{SV}. This coefficient takes into account the contraction of flow. Defining the flow coefficient c_{SV} as the function of the radial clearance RC and the Reynolds number Re allows for unambiguous determination of its value in multi-tooth segments. It means that this model can be used for geometries of segments of straight and staggered seals of various number of teeth and axial direction of gas flow. Presented model enables determination of theoretical, minimum gas mass flow in multi-tooth segments of a wide range of radial clearance. Value of this flux results from the assumption of the gas expansion in gaps and total dissipation of kinetic energy in seal chambers. Comparing the value of real mass flow with the value obtained with the use of calculation model enables determination of the segment leakage rate and determination of the kinetic energy carry-over coefficient for the investigated geometries.

Presented model creates a new method for determination of the kinetic energy carry-over coefficient which depends not only on the seal geometry but also on the pressure drop of gas in the seal.

Therefore, the mass flow determined with the use of our model is the measure of theoretical seal tightness. Proposed model allows for determining the distribution of pressure and other parameters along the segment length.

REFERENCES

Asako, Y., K. Nakayama, and T. Shinozuka. (2005). Effect of Compressibility on Gaseous Flows in a Micro-Tube. *International Journal of Heat and Mass Transfer* 48(23–24),4985–94.

Asok, S. P., K. Sankaranarayanasamy, T. Sundararajan, K. Rajesh, and G. Sankar Ganeshan (2007). Neural Network and CFD-

Based Optimisation of Square Cavity and Curved Cavity Static Labyrinth Seals. *Tribology International* 40(7),1204–16.

Childs, Dara W. and J. K. Scharrer (1986). An Iwatsubo-Based Solution for Labyrinth Seals: Comparison to Experimental Results. *Journal of Engineering for Gas Turbines and Power* 108(2),325–31.

Dereli, Yilmaz and Dursun Eser (2004). Flow Calculations in Straight-through Labyrinth Seals by Using Moody's Friction-Factor Model. *Mathematical and Computational Applications* 9(3),435–42.

Egli, Adolf. (1935). The Leakage of Steam through Labyrinth Seals. *Trans. ASME* 57,115–22.

Hodkinson, B. (1939). Estimation of the Leakage through a Labyrinth Gland. *Proceedings of the Institution of Mechanical Engineers* 141(1),283–88.

Hong, C., Y. Asako, K. Suzuki, and M. Faghri. (2012). Friction Factor Correlations for Compressible Gaseous Flow in a Concentric Micro Annular Tube. *Numerical Heat Transfer; Part A: Applications* 61(3),163–79.

Hu, D., L. Jia, and L. Yang. (2014). Dimensional Analysis on Resistance Characteristics of Labyrinth Seals. *Journal of Thermal Science* 23(6),516–22.

Joachimiak, D., M. Joachimiak, and P. Krzyślak. (2012). Description Program Dławnica Used for Calculations Labyrinth Seals." *Journal of Mechanical and Transport Engineering* 65(1),25–35.

Joachimiak, D.and P. Krzyślak. (2016). A Model of Gas Flow with Friction in a Slotted Seal. *Archives of Thermodynamics* 37(3),95–108.

Joachimiak, Damian and Piotr Krzyślak (2017). "Experimental Research and CFD Calculations Based Investigations Into Gas Flow in a Short Segment of a Heavily Worn Straight Through Labyrinth Seal. *Polish Maritime Research* 24(2),83–88.

Joachimiak, Damian and Piotr Krzyślak (2019). The Analysis of the Gas Flow in a Labyrinth Seal of Variable Pitch. *Journal of Applied Fluid Mechanics* 12(4).

Kawashima, D. and Y. Asako. (2014). Data Reduction of Friction Factor of Compressible Flow in Micro-Channels. *International Journal of Heat and Mass Transfer* 77,257–61.

Lampart, P. (2009). Invetigation of Endwall Flows and Losses in Axial Turbines Part I: Formation of Endwall Flows and Losses. *Journal of Theoretical and Applied Mechanics* 47(2),321–42.

Martin, H. M. (1908). Labyrinth Packings. *Engineering* 85(10),35–38.

Melnik, V. A. (2013). Computed Universal Dependence for Determining Leakage of Media Through Groove Seals. *Chemical and Petroleum Engineering* 48(11–12),751–59.

Scharrer, J. K. (1988). Theory versus Experiment for the Rotordynamic Coefficients of Labyrinth Gas Seals: Part I—A Two Control Volume Model. *Journal of Vibration Acoustics Stress and Reliability in ….*

Szymanski, Artur, Wlodzimierz Wróblewski, Daniel Fraczek, Krzysztof Bochon, Slawomir Dykas, and Krzysztof Marugi. (2018). "Optimization of the Straight-Through Labyrinth Seal With a Smooth Land." *Journal of Engineering for Gas Turbines and Power* 140(12),122503.

Trütnovsky, Karl. (1964). *Noncontacting Seals; Basics and Applications of Slot and Labyrinth Fluid-Flow Seals*. VDI-Verlag bh Dusseldorf, Publishing House of the Association of German Engineers.

Wang, Wei-zhe, Ying-zheng Liu, Pu-ning Jiang, and Han-ping Chen. (2007). Numerical Analysis of Leakage Flow through Two Labyrinth Seals. *Journal of Hydrodynamics* 19(1),107–12.

Yuan, Haomin, Sandeep Pidaparti, Mathew Wolf, John Edlebeck, and Mark Anderson. (2015). "Numerical Modeling of Supercritical Carbon Dioxide Flow in See-through Labyrinth Seals. *Nuclear Engineering and Design* 293,436–46.

Zhang, Wan Fu, Jian Gang Yang, Chun Li, and Yong Wei Tian. (2014). Comparison of Leakage Performance and Fluid-Induced Force of Turbine Tip Labyrinth Seal and a New Kind of Radial Annular Seal. *Computers and Fluids* 105,125–37.

Zhirong, Lin, Wang Xudong, Yuan Xin, Shibukawa Naoki, and Noguchi Taro. (2015). Investigation and Improvement of the Staggered Labyrinth Seal. *Chinese Journal of Mechanical Engineering* 28(2),402–8.

Zimmermann, H. and K. H. Wolff. (1987). Comparison Between Empirical and Numerical Labyrinth Flow Correlations. *American Society of Mechanical Engineers (Paper)* 87-GT-86,1–6.